

Transverse Compressional Damping in the Vibratory Response of Elastic-Viscoelastic-Elastic Beams

B. E. Douglas*

David W. Taylor Naval Ship Research and Development Center, Annapolis, Md.

and

J. C. S. Yang†

University of Maryland, College Park, Md.

The effects of transverse compressional damping in the vibratory response of three-layer elastic-viscoelastic-elastic beams are considered both analytically and experimentally in a mechanical impedance format. The relative importance of this type of damping is assessed through comparison with the shear damping mechanism inherent in the composite using the Mead and Markus model. Results of this investigation suggest that the effects from transverse compressional damping have a relatively narrow frequency bandwidth dependent on the elastic loss tangent of the damping core and are centered at the compressional (delamination) frequency ω_c of the composite. Compressional damping is shown to have a minimal effect on the transverse dynamic response of thin three-layer damped beams for frequencies significantly less than ω_c where a shear damping model provides a more accurate prediction of the composite loss factor.

Nomenclature

$w(x)$	= transverse displacement
$u(x)$	= longitudinal displacement
i	= $\sqrt{-1}$
m	= mass per unit length
ℓ	= beam length
t_v	= thickness of viscoelastic core
t_i	= thickness of i th layer
b	= beam width
E_i	= elastic (Young's) modulus of i th layer
ρ_i	= mass per unit length of i th layer
$E_v^*(\omega)$	= $E_v (1 + i\delta)$ = complex dynamic elastic modulus of viscoelastic core
E_v	= elastic storage modulus of viscoelastic core
δ	= elastic loss tangent of viscoelastic core
$G_v^*(\omega)$	= $G_v (1 + i\beta)$ = complex dynamic shear modulus of viscoelastic core
G_v	= shear storage modulus of viscoelastic core
β	= shear loss tangent of viscoelastic core
ω	= radial frequency
I_i	= moment of inertia of i th layer
k^*	= compressional spring constant per unit length = $E_v^* b / t_v$
ω_c	= compressional composite frequency
$Z(x, \omega)$	= mechanical impedance of beam
P_0	= applied force

Introduction

IN recent years, the dynamic design of structures has received increased emphasis as current standards for noise radiation, machinery reliability, and structural fatigue have required increased attention to vibration control while maintaining or reducing structural weight and size. This trend is particularly noticeable in the design of modern aerospace vehicles where high performance standards for speed, maneuverability, and payload have motivated research into

the development of lightweight inherently damped structures. The damping in such structures is utilized primarily to control structural damage from fatigue, as well as cabin noise detrimental to health and speech intelligibility, and to reduce the chance of machinery and electrical equipment failure from operation in a dynamic environment.

The transverse vibratory response of elastic-viscoelastic-elastic laminated beams has received considerable attention since Plass¹ and Kerwin² examined the potential of this composite in vibration control. Many investigators¹⁻⁸ have studied the dynamic response of the three-layer damped sandwich beam, concentrating predominantly on the broadband damping inherent in the composite associated with shear damping. In a classic paper² on this subject, Kerwin analyzed the shear damping in an infinitely long, simply supported beam with a soft viscoelastic core and a thin, stiff constraining layer, deriving an expression for the complex flexural stiffness of the beam section. DiTaranto³ extended Kerwin's work, deriving a sixth-order differential equation of motion in terms of dynamic longitudinal beam displacement $u(x)$. In a later paper, Mead and Markus⁴ derived a sixth-order differential equation in terms of the transverse motion of the beam, which is an important factor in experimentally validating the model. In the same paper, Mead and Markus also examined the form of the boundary constraints on the composite for many widely used end conditions and showed that the eigenvalues for such a system are generally complex for boundary conditions other than simply supported. Lu and Douglas⁶ evaluated the Mead and Markus model in several experiments which showed that this model adequately predicted the damped resonance frequencies and damping inherent in the low-order modes of two relatively thin three-layer laminates.

An important feature of the aforementioned work was the assumption that transverse displacements, $w(x)$, of all points on a cross-section are equal. For thin composites where the product of the viscoelastic layer thickness and the constraining layer thickness is small, shear damping appears to be the major factor controlling the resonance response of these beams in the audio-frequency spectrum. However, as the thickness of soft ($E_v < 10^8$ N/m²) viscoelastic cores and constraining layer increase, compressional damping can be expected to play an increasingly important role in the dynamic response of such structures. This paper examines, both

Received Sept. 20, 1977; revision received May 16, 1978. Copyright © American Institute of Aeronautics and Astronautics, Inc., 1978. All rights reserved.

Index categories: Vibration; Structural Dynamics; Structural Composite Materials.

*Physicist.

†Professor, Mechanical Engineering Department.

analytically and experimentally, the contribution of compressional damping on the transverse dynamic response of the three-layer damped beam and compares the importance of this form of damping with shear damping using the aforementioned model developed by Mead and Markus. The intent is to help provide design insight for the utilization of such composites for possible application to beam-like vehicular appendages or to machinery or instrument mounting structures.

Analytical Formulation

The three-layer damped beam consists of two elastic face layers separated by a thin, relatively soft viscoelastic damping core. Figure 1 depicts the geometry and coordinate system utilized in this paper. The case of fixed-free (cantilever) boundary constraints is considered with a concentrated sinusoidal load $P_0 e^{i\omega t}$ applied at the free end to facilitate comparison between analytical and experimentally derived spectra. The dynamic response of this composite is examined in a mechanical impedance format. The complex elastic and shear moduli are assumed both temperature and frequency dependent, and the loss tangents of the elastic layers are assumed negligible. No restrictions are placed on the densities and moduli of the layers, except that the viscoelastic layer is considered soft compared to the elastic layers, i.e., $E_v \ll E_i$, and its mass is negligible. The elastic layers need not be identical. The time-dependant equations of motion discussed in this paper assume steady-state harmonic displacements.

Compressional Damping Model

The equations of motion for the three-layer damped laminate depicted in Fig. 1 and based only on compressional damping are derived assuming that 1) the viscoelastic damping core is linear and relatively soft, so that it can be modeled as a complex compression spring; and 2) the rotary inertia and shear deformation of the elastic layers are negligible, so that the Bernoulli-Euler beam theory can be employed. With these assumptions, the equations of motion for this composite can be written as two coupled fourth-order partial differential equations:

$$-E_1 I_1 \frac{\partial^4 w_1}{\partial x^4} = k^* (w_1 - w_3) + \rho_1 \frac{\partial^2 w_1}{\partial t^2} \quad (1a)$$

$$-E_3 I_3 \frac{\partial^4 w_3}{\partial x^4} = k^* (w_3 - w_1) + \rho_3 \frac{\partial^2 w_3}{\partial t^2} \quad (1b)$$

Assuming harmonic time dependence, these equations can be combined into a single eighth-order differential equation with complex coefficients for the base cantilever beam (i.e., layer 1):

$$\frac{d^8 w_1(x)}{dx^8} + \left[\frac{k^* - \rho_1 \omega^2}{E_1 I_1} + \frac{k^* - \rho_3 \omega^2}{E_3 I_3} \right] \frac{d^4 w_1(x)}{dx^4} + \left[\frac{\rho_3 \rho_1 \omega^4 - k^* \omega^2 (\rho_1 + \rho_3)}{E_1 I_1 E_3 I_3} \right] w_1(x) = 0 \quad (2)$$

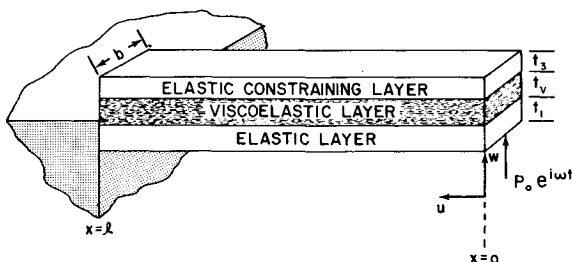


Fig. 1 Geometry and coordinate system for the three-layer damped sandwich beam.

The response of the constraining layer can be written in terms of the response of the cantilever beam as

$$w_3(x) = \frac{k^* - \rho_1 \omega^2}{k^*} w_1(x) + E_1 I_1 \frac{d^4 w_1}{dx^4} \quad (3)$$

Using a progressive wave approach, the solution for Eq. (2) can be written in terms of the complex wave numbers ϵ and μ as

$$w_1(x) = A_1 e^{\epsilon x} + A_2 e^{-\epsilon x} + A_3 e^{i\mu x} + A_4 e^{-i\mu x} + A_5 e^{\mu x} + A_6 e^{-\mu x} + A_7 e^{i\mu x} + A_8 e^{-i\mu x} \quad (4a)$$

$$w_3(x) = M[A_1 e^{\epsilon x} + A_2 e^{-\epsilon x} + A_3 e^{i\mu x} + A_4 e^{-i\mu x}] + N[A_5 e^{\mu x} + A_6 e^{-\mu x} + A_7 e^{i\mu x} + A_8 e^{-i\mu x}] \quad (4b)$$

where

$$\epsilon = \left[-\frac{\alpha}{2} - \left(\frac{\alpha^2}{4} - \eta \right)^{1/2} \right]^{1/4}, \quad \mu = \left[-\frac{\alpha}{2} + \left(\frac{\alpha^2}{4} - \eta \right)^{1/2} \right]^{1/4}$$

$$\alpha = \frac{k^* - \rho_1 \omega^2}{E_1 I_1} + \frac{k^* - \rho_3 \omega^2}{E_3 I_3}, \quad \eta = \frac{\rho_1 \rho_3 \omega^4 - k^* \omega^2 (\rho_1 + \rho_3)}{E_1 I_1 E_3 I_3}$$

$$M = \left[\frac{k^* - \rho_1 \omega^2}{k^*} + E_1 I_1 \epsilon^4 \right], \quad N = \left[\frac{k^* - \rho_1 \omega^2}{k^*} + E_1 I_1 \mu^4 \right]$$

For fixed-free boundary conditions, the four equations of constraint for layer 1 require

$$w_1(0) = 0; \quad \left. \frac{\partial w_1}{\partial x} \right|_{x=0} = 0; \quad \left. \frac{\partial^2 w_1}{\partial x^2} \right|_{x=0} = 0; \quad \left. \frac{\partial^3 w_1}{\partial x^3} \right|_{x=0} = \frac{P_0}{E_1 I_1} e^{i\omega t} \quad (5)$$

As indicated the applied concentrated sinusoidal loading is accounted for implicitly in the shear boundary constraint at $x=0$.

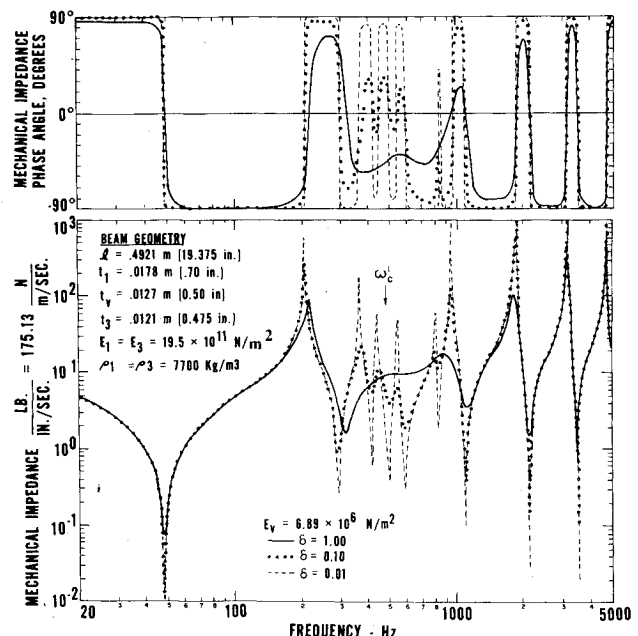


Fig. 2 Transverse driving point mechanical impedance and phase spectrum for a three-layer damped beam ($E_v = 1000$ psi): compressional damping model.

The four boundary constraints for layer 3 require

$$\frac{\partial^2 w_3}{\partial x^2} = 0; \quad \frac{\partial^3 w_3}{\partial x^3} = 0 \text{ at } x=0 \text{ and } x=\ell \quad (6)$$

The shear condition evolved from assuming that the effective shear force $\delta k_{\text{eff}} (\omega_3 - \omega_1)$ transmitted by the viscoelastic layer at the ends of the laminate is zero; i.e.,

$$\lim_{\delta A \rightarrow 0} \delta k_{\text{eff}} - \lim_{\delta A \rightarrow 0} \left(\frac{E_v^* \delta A}{t_v} \right) = 0$$

These equations of constraint can be placed in a matrix representation to solve for the complex coefficients A_n by standard matrix inversion methods or $[M] \cdot [A] = [P]$:

ϵ^3	$-\epsilon^3$	$-i\epsilon^3$	$i\epsilon^3$	μ^3	$-\mu^3$	$-i\mu^3$	$i\mu^3$
ϵ^2	ϵ^2	$-\epsilon^2$	$-\epsilon^2$	μ^2	μ^2	$-\mu^2$	$-\mu^2$
$e^{\epsilon\ell}$	$e^{-\epsilon\ell}$	$e^{i\epsilon\ell}$	$e^{-i\epsilon\ell}$	$e^{\mu\ell}$	$e^{-\mu\ell}$	$e^{i\mu\ell}$	$e^{-i\mu\ell}$
$\epsilon e^{\epsilon\ell}$	$-\epsilon e^{-\epsilon\ell}$	$i\epsilon e^{i\epsilon\ell}$	$-i\epsilon e^{-i\epsilon\ell}$	$\mu e^{\mu\ell}$	$-\mu e^{-\mu\ell}$	$i\mu e^{i\mu\ell}$	$-i\mu e^{-i\mu\ell}$
$M\epsilon^2$	$M\epsilon^2$	$-M\epsilon^2$	$-M\epsilon^2$	$N\mu^2$	$N\mu^2$	$-N\mu^2$	$-N\mu^2$
$M\epsilon^3$	$-M\epsilon^3$	$-iM\epsilon^3$	$iM\epsilon^3$	$N\mu^3$	$-N\mu^3$	$-iN\mu^3$	$iN\mu^3$
$M\epsilon^2 e^{\epsilon\ell}$	$M\epsilon^2 e^{-\epsilon\ell}$	$-M\epsilon^2 e^{i\epsilon\ell}$	$-M\epsilon^2 e^{-i\epsilon\ell}$	$N\mu^2 e^{\mu\ell}$	$N\mu^2 e^{-\mu\ell}$	$-N\mu^2 e^{i\mu\ell}$	$-N\mu^2 e^{-i\mu\ell}$
$M\epsilon^3 e^{\epsilon\ell}$	$-M\epsilon^3 e^{-\epsilon\ell}$	$-iM\epsilon^3 e^{i\epsilon\ell}$	$iM\epsilon^3 e^{-i\epsilon\ell}$	$N\mu^3 e^{\mu\ell}$	$-N\mu^3 e^{-\mu\ell}$	$-iN\mu^3 e^{i\mu\ell}$	$iN\mu^3 e^{-i\mu\ell}$

$$\begin{bmatrix} A_1 \\ A_2 \\ A_3 \\ A_4 \\ A_5 \\ A_6 \\ A_7 \\ A_8 \end{bmatrix} = \begin{bmatrix} P_0/E_1 I_1 \\ 0 \\ 0 \\ 0 \\ 0 \\ 0 \\ 0 \\ 0 \end{bmatrix} \quad (7)$$

These coefficients then can be determined at each frequency of concern by multiplying the inverse of the constraint matrix $[M]$ and the loading matrix $[P]$. From this information, the mechanical impedance at any arbitrary point on the surface of the cantilever beam (layer 1) can then be written as

$$Z_1(x, \omega) = (P_0/i\omega) [A_1 e^{\epsilon x} + A_2 e^{-\epsilon x} + A_3 e^{i\epsilon x} + A_4 e^{-i\epsilon x} + A_5 e^{\mu x} + A_6 e^{-\mu x} + A_7 e^{i\mu x} + A_8 e^{-i\mu x}] - I$$

and the transfer impedance to layer 3 as

$$Z_3(x, \omega) = (P_0/i\omega) \{ M[A_1 e^{\epsilon x} + A_2 e^{-\epsilon x} + A_3 e^{i\epsilon x} + A_4 e^{-i\epsilon x}] + N[A_5 e^{\mu x} + A_6 e^{-\mu x} + A_7 e^{i\mu x} + A_8 e^{-i\mu x}] \} - I$$

From the analytical model just described, the dynamic response of a damped three-layer laminated beam containing only compressional damping can be studied by examining the mechanical impedance spectra of several beam geometries and material properties. Figure 2 shows the mechanical impedance spectra generated from this model of a selected case: a steel laminate with geometry outlined in the figure, and a viscoelastic damping core with an elastic storage modulus of $6.89 \times 10^6 \text{ N/m}^2$ (1000 lb-in.⁻²) and several values of elastic

loss tangent. As is evident from this figure, the damping in this composite is negligible except for the spectral region between 250 and 2000 Hz centered at 500 Hz. In this region, the damping is strongly dependent on the elastic loss tangent. This result can be anticipated from consideration of a model that treats the face layers as lumped masses and the viscoelastic layer as a complex distributed spring. This model gives rise to a compressional frequency inherent in composite working to delaminate the face layers:

$$\omega_c^* = \left[\left(\frac{E_v^*}{t_v \ell} \right) \left(\frac{1}{\rho_1 t_1} + \frac{1}{\rho_3 t_3} \right) \right]^{1/2} = \omega_c' (1 + i\delta)^{1/2}$$

Since, according to this model, the viscoelastic layer receives the greatest dynamic compressional strains in this spectral

region, which, in turn, is the primary mechanism converting vibratory energy to heat, it is to be expected that vibrational modes of the composite occurring near this frequency would exhibit a high degree of damping for high-loss viscoelastic materials.

Shear Damping Model

The equation for transverse motion for the three-layer damped laminate based only on shear damping was derived by Mead and Markus⁴ assuming that 1) the shear strain is constant across the depth of the damping core, which is linearly viscoelastic; 2) shear strains in the face plates and longitudinal stresses in the core are negligible; 3) transverse direct strains in the core and face plates are negligible, so that transverse displacements of all points on a beam cross section are equal; and 4) the shear stress in the core acts uniformly between the midplanes of the face plates. From these assumptions, a sixth-order partial differential equation for the damped laminate subjected to a concentrated sinusoidal loading was derived⁴ in terms of the transverse displacement variable w :

$$\frac{\partial^6 w}{\partial x^6} - g(1 + Y) \frac{\partial^4 w}{\partial x^4} + \frac{m}{D_t} \frac{\partial^4 w}{\partial x^2 \partial t^2} = \frac{mg}{D_t} \frac{\partial^2 w}{\partial t^2} \quad (8)$$

where

$$g = \frac{G_v^*}{t_v} \left(\frac{1}{E_1 t_1} + \frac{1}{E_3 t_3} \right)$$

$$Y = \frac{d^2}{D_t} \left(\frac{E_1 t_1 E_3 t_3}{E_1 t_1 + E_3 t_3} \right)$$

$$d = t_v + \frac{1}{2}(t_1 + t_3)$$

$$D_t = \frac{(E_1 t_1^3 + E_3 t_3^3) b}{12}$$

Again, a progressive wave solution for this equation can be written in terms of the complex wave numbers δ_1 , δ_2 , and δ_3 :

$$w(x) = C_1 e^{\delta_1 x} + C_2 e^{-\delta_1 x} + C_3 e^{\delta_2 x} + C_4 e^{-\delta_2 x} + C_5 e^{\delta_3 x} + C_6 e^{-\delta_3 x} \quad (9)$$

$$\begin{bmatrix} \delta_1^3 & -\delta_1^3 & \delta_2^3 & -\delta_2^3 & \delta_3^3 & -\delta_3^3 \\ \delta_1^2 & \delta_1^2 & \delta_2^2 & \delta_2^2 & \delta_3^2 & \delta_3^2 \\ R_1 & R_1 & R_2 & R_2 & R_3 & R_3 \\ e^{\delta_1 \ell} & e^{-\delta_1 \ell} & e^{\delta_2 \ell} & e^{-\delta_2 \ell} & e^{\delta_3 \ell} & e^{-\delta_3 \ell} \\ \delta_1 e^{\delta_1 \ell} & -\delta_1 e^{-\delta_1 \ell} & \delta_2 e^{\delta_2 \ell} & -\delta_2 e^{-\delta_2 \ell} & \delta_3 e^{\delta_3 \ell} & -\delta_3 e^{-\delta_3 \ell} \\ S_1 e^{\delta_1 \ell} & -S_1 e^{-\delta_1 \ell} & S_2 e^{\delta_2 \ell} & -S_2 e^{-\delta_2 \ell} & S_3 e^{\delta_3 \ell} & -S_3 e^{-\delta_3 \ell} \end{bmatrix} \cdot \begin{bmatrix} C_1 \\ C_2 \\ C_3 \\ C_4 \\ C_5 \\ C_6 \end{bmatrix} = \begin{bmatrix} P_0/D_t \\ 0 \\ 0 \\ 0 \\ 0 \\ 0 \end{bmatrix} \quad (11)$$

where

$$\delta_1 = [\gamma_1 + \gamma_2 - (g/3)(I + Y)]^{1/2}$$

$$\delta_2 = \left[-\left(\frac{\gamma_1 + \gamma_2}{2} \right) + i \left(\frac{\gamma_1 - \gamma_2}{2} \right) \sqrt{3} - \frac{g}{3}(I + Y) \right]^{1/2}$$

$$\delta_3 = \left[-\left(\frac{\gamma_1 + \gamma_2}{2} \right) - i \left(\frac{\gamma_1 - \gamma_2}{2} \right) \sqrt{3} - \frac{g}{3}(I + Y) \right]^{1/2}$$

$$\gamma_1 = \left[-\frac{\xi_2}{2} + \left(\frac{\xi_2^2}{4} + \frac{\xi_1^3}{27} \right)^{1/2} \right]^{1/2}$$

$$\gamma_2 = \left[-\frac{\xi_2}{2} - \left(\frac{\xi_2^2}{4} + \frac{\xi_1^3}{27} \right)^{1/2} \right]^{1/2}$$

$$\xi_1 = -(m\omega^2/D_t) - \frac{1}{3}g^2(I + Y)^2$$

$$\xi_2 = (m\omega^2/D_t)g - \frac{1}{3}g(I + Y)(m\omega^2/D_t) - (2/27)g^3(I + Y)$$

For cantilever end conditions, the equations of constraint require, at the free end, the moment χ to be zero or

$$\chi = \frac{D_t}{g} \left(-\frac{\partial^4 w}{\partial x^4} + g(I + Y) \frac{\partial^2 w}{\partial x^2} + \frac{m\omega^2}{D_t} w \right) = 0$$

and the shear force $S = \partial \chi / \partial x$ to equal the applied concentrated force or

$$S = \frac{D_t}{g} \left(-\frac{\partial^5 w}{\partial x^5} + g(I + Y) \frac{\partial^3 w}{\partial x^3} + \frac{m\omega^2}{D_t} \frac{\partial w}{\partial x} \right) = P_0 e^{i\omega t}$$

and the longitudinal face plate displacement $u(x)$ to be unrestrained. These conditions reduce to the simple form at $x=0$:

$$\frac{\partial^2 w}{\partial x^2} = 0; \quad \frac{\partial^3 w}{\partial x^3} = \frac{P_0}{D_t} e^{i\omega t}; \quad \frac{\partial^4 w}{\partial x^4} - \frac{m\omega^2}{D_t} w = 0$$

At the fixed end, the equations of constraint require

$$w(\ell) = 0; \quad \frac{\partial w}{\partial x} \Big|_{x=\ell} = 0; \quad u(\ell) = 0$$

The longitudinal displacement can be described in terms of the transverse displacement for a concentrated dynamic load by the expression

$$u(x) = \left(\frac{-D_t}{E_1 t_1 d} \right) \left[\frac{1}{g^2} \frac{\partial^5 w}{\partial x^5} - \frac{Y}{g} \frac{\partial^3 w}{\partial x^3} - \left(\frac{m\omega^2}{D_t g^2} + Y \right) \frac{\partial w}{\partial x} \right] \quad (10)$$

These equations can be placed in a matrix representation and solved for the complex coefficients C_n in a manner similar to that described in the compressional damping model:

where

$$R_1 = \delta_1^4 - (m\omega^2/D_t)$$

$$R_2 = \delta_2^4 - (m\omega^2/D_t)$$

$$R_3 = \delta_3^4 - (m\omega^2/D_t)$$

$$S_1 = \frac{\delta_1^5}{g^2} - \frac{Y}{g} \delta_1^3 - \left(\frac{m\omega^2}{D_t g^2} + Y \right) \delta_1$$

$$S_2 = \frac{\delta_2^5}{g^2} - \frac{Y}{g} \delta_2^3 - \left(\frac{m\omega^2}{D_t g^2} + Y \right) \delta_2$$

$$S_3 = \frac{\delta_3^5}{g^2} - \frac{Y}{g} \delta_3^3 - \left(\frac{m\omega^2}{D_t g^2} + Y \right) \delta_3$$

Upon determining the C_n coefficients by matrix inversion, the mechanical impedance at an arbitrary point on the laminate can be calculated from the expression

$$Z(x, \omega) = (P_0/i\omega) (C_1 e^{\delta_1 x} + C_2 e^{-\delta_1 x} + C_3 e^{\delta_2 x} + C_4 e^{-\delta_2 x} + C_5 e^{\delta_3 x} + C_6 e^{-\delta_3 x}) - i$$

Previous papers^{4,6} on this subject have shown that shear damping is a broadband phenomenon strongly dependent on the shear loss tangent of the viscoelastic layer.

Experimental Evaluation

Three damped sandwich beams were constructed to serve to evaluate the relative importance of compressional and shear damping in elastic-viscoelastic-elastic beams. Two beams were designed with the compressional frequency, ω_c , located in the 20- to 5000-Hz spectrum, and a third beam was designed with ω_c above 5000 Hz. The elastic face layers of all beams were constructed from steel. Specimens 1 and 2 incorporated an acrylic base viscoelastic material with a complex dynamic shear modulus in the 20- to 5000-Hz spectral region which can be approximated (assuming ther-

moheologically simple material behavior) at a temperature of 22°C by the expressions

$$G_v = (1.42 \times 10^5) \exp[0.494 \ln(\omega/2\pi)] \text{ N/m}^2 \quad (12a)$$

$$\beta = 1.46 \quad (12b)$$

Specimen 1 contained a viscoelastic layer thickness of 0.00686 m which placed its composite compressional frequency near 900 Hz, and specimen 2 contained a viscoelastic layer thickness of 0.000102 m which placed its composite compressional frequency outside the spectral range of the experiments reported herein. The complex dynamic elastic modulus used to generate the analytical compressional damping spectrum for specimen 1 was obtained from assuming incompressibility and a real Poisson ratio (i.e., $E_v = 3G_v$ and $\delta = \beta$).

Specimen 3 incorporated a medium-density, closed-cell, neoprene foam layer with a complex dynamic elastic modulus that can be approximated at a temperature of 22°C by the expressions

$$E_v = 1.078 \times 10^5 \exp[0.4041 \ln(\omega/2\pi)] \text{ N/m}^2 \quad (13a)$$

$$\delta = \begin{cases} 0.8, & 20 \text{ Hz} < \omega/2\pi < 60 \text{ Hz} \\ 10.47 \exp[-0.628 \ln(\omega/2\pi)], & 60 \text{ Hz} < \omega/2\pi < 150 \text{ Hz} \\ 0.45, & 150 \text{ Hz} < \omega/2\pi < 500 \text{ Hz} \end{cases} \quad (13b)$$

The complex dynamic elastic modulus of the neoprene foam [Eqs. (13)] was obtained from a series of resonance mass-spring experiments. The measurements to determine the expressions in Eqs. (12) were obtained⁹ from a commercial apparatus that utilizes dynamic stress-strain and related phase angle measurements. The thickness of the foam layer was 0.0127 m. The compressional frequency of this composite is located near 200 Hz.

The cantilever test fixture used to mount these beams was evaluated by comparing the measured mechanical impedance of an undamped simple beam with Bernoulli-Euler theory. Figure 3 shows the 20-5000-Hz mechanical impedance spectrum of a steel beam 0.0178 m thick, 0.0508 m wide, and 0.4921 m long. With this test fixture, excellent agreement was observed between measurement and theory as to values for both resonance and antiresonance frequencies. The dynamic range between associated resonance-antiresonance pairs for the measured steel beams spectrum exceeds 40 dB throughout the 20- to 5000-Hz spectrum, increasing to in excess of 100dB for the low-order vibrational modes. All measured spectra

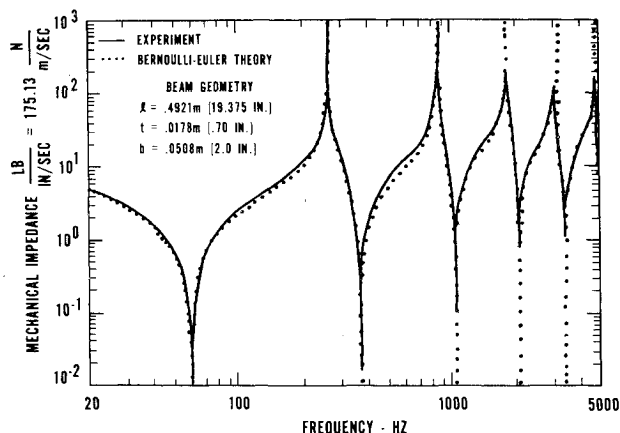


Fig. 3 Transverse driving point mechanical impedance spectrum of an elastic beam: evaluation of experimental boundary conditions and instrumentation.

discussed in this paper were obtained from transducers that had a negligible mass loading (<0.004 kg) effect on the structure. The experimental results were obtained using a swept sine wave and analog impedance instrumentation with crystal tracking filters. Two transducer mounting arrangements were used as a check for accuracy. The impedance spectra presented herein were obtained using the reaction mass impedance measurement method, where an electromagnetic vibration generator was mounted to the test specimen via a small pin drive rod, and an accelerometer was mounted on the reaction mass of the shaker to monitor dynamic force. The second transducer mounting arrangement used the traditional mechanical impedance head, where a piezoelectric crystal is placed in compression between the vibration generator and the test specimen. Since the reaction mass method possessed a greater dynamic range over a wider frequency range, it was selected as the experimental analysis

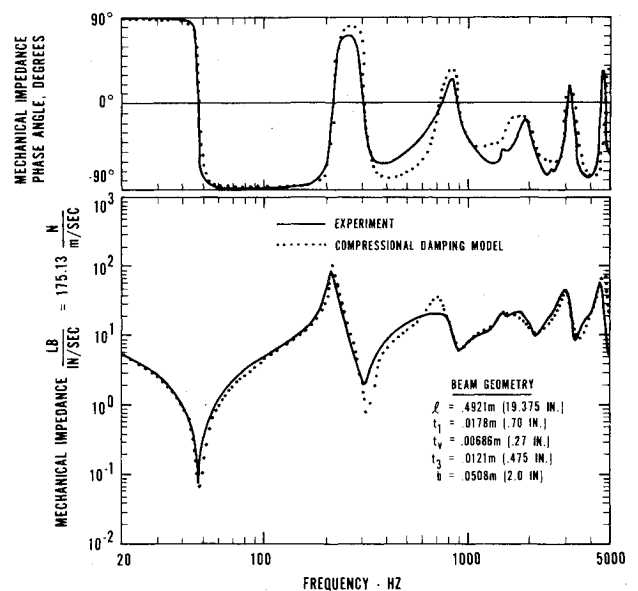


Fig. 4 Transverse driving point mechanical impedance and phase angle spectrum for specimen 1.

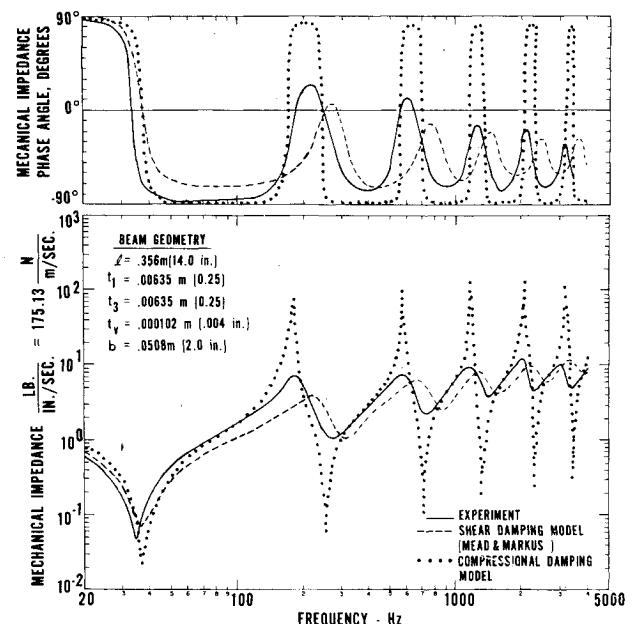


Fig. 5 Transverse driving point mechanical impedance and phase angle spectrum for specimen 2.

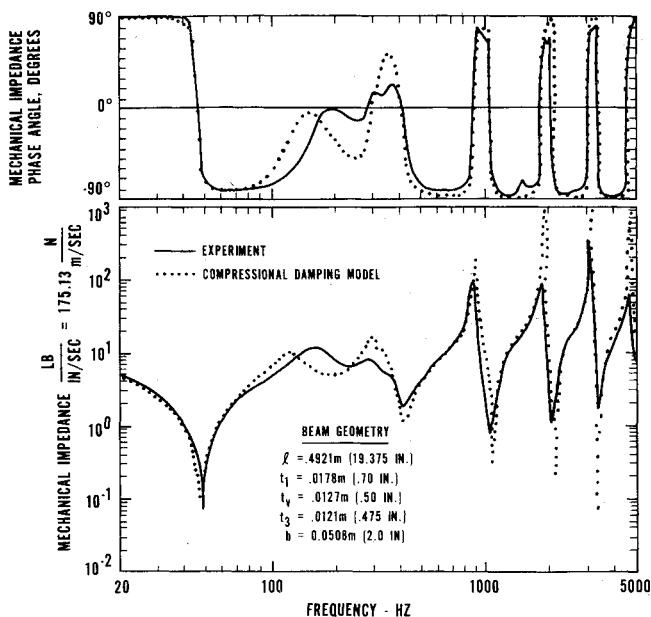


Fig. 6 Transverse driving point mechanical impedance and phase angle spectrum for specimen 3.

procedure for this investigation. Using the method just described, a 20-5000 Hz mechanical impedance and associated phase angle spectrum was obtained for test specimens 1-3, which are presented in Figs. 4-6, respectively.

Discussion

The utilization of structural damping methods to control dynamic structural response has become increasingly widespread in recent years because of increased performance standards for vehicles, as well as stricter environmental standards. Constrained layer damping is a major proven structural damping technique with high damping efficiencies. This paper has attempted to isolate the major damping mechanisms inherent in constrained composites in order to ascertain their potential and provide some insight into the effective design of such structures. For this reason, a cantilever beam configuration was selected, together with a comparison of individual analytical models incorporating only one of the major damping mechanisms.

As the results indicate in Figs. 2, 4, and 6, transverse compressional damping can provide significant attenuation in the vibrational energy of resonant structures in a narrow frequency band centered at the compressional frequency of the composite. In addition, the elastic loss tangent of the viscoelastic layer is an important factor controlling the bandwidth and amount of effective vibratory attenuation. Examination of Fig. 6 demonstrates that, for frequencies significantly removed from ω_c , compressional damping provides little attenuation to the dynamic structural response.

Within the stated assumptions, the model developed for compressional damping in this paper provided excellent

agreement with the measured data in the spectral regions governed by this mechanism. Finally, additional support for the Mead and Markus model of shear damping was provided by the agreement observed between experiment and theory for specimen 2, especially the mechanical impedance magnitude and relative bandwidth near the resonance frequencies of the composite, which is a measure of the modal damping inherent in the structure. A small difference was noted in the prediction of the resonance frequencies between experiment and the shear damping model for specimen 2. This shift was attributed to the high stiffness of the constraining layer in this specimen in relation to that of the damping core, which favors dynamic delamination. In addition, shear deformation and rotary inertia effects were neglected in the shear model. It is concluded that shear damping is a broadband mechanism, which, for most engineering purposes and commercially available damping materials, adequately describes the damping inherent in the transverse dynamic response of thin elastic-viscoelastic-elastic beams outside the spectral influence of compressional effects. Inside this spectral band, the relative displacement between the elastic face layers of the composite must be considered in dynamic calculations.

Acknowledgment

This work is based on the initial phases of a dissertation by the first author toward partial fulfillment of the requirements of a Ph.D. degree from the Mechanical Engineering Department of the University of Maryland. All opinions or assertions made in this paper are those of the authors and not to be construed as official or necessarily reflecting the views of the Navy or the naval service at large.

References

- ¹Plass, H. J., Jr., "Damping of Vibrations in Elastic Rods and Sandwich Structures by Incorporation of Additional Visco-Elastic Material," *Proceedings of the Third Midwestern Conference on Solid Mechanics*, Univ. of Michigan, April 1957, pp. 43-71.
- ²Kerwin, E. M., Jr., "Damping of Flexural Waves by a Constrained Visco-Elastic Layer," *Journal of the Acoustical Society of America*, Vol. 31, July 1959, pp. 952-962.
- ³DiTaranto, R. A., "Theory of Vibratory Bending for Elastic and Viscoelastic Layered Finite-Length Beams," *Journal of Applied Mechanics*, Vol. 87, Ser. E, Dec. 1965, pp. 861-867.
- ⁴Mead, D. J. and Markus, S., "The Forced Vibration of a Three-Layer, Damped Sandwich Beam with Arbitrary Boundary Conditions," *Journal of Sound and Vibration*, Vol. 10, Feb. 1969, pp. 163-175.
- ⁵Mead, D. J. and DiTaranto, R. A., "Resonance Response Criteria of a Damped Three-Layered Beam," *Journal of Engineering for Industry*, Vol. 94, Ser. B, Feb. 1972, pp. 174-180.
- ⁶Lu, Y. P. and Douglas, B. E., "On the Forced Vibrations of Three-Layer Damped Sandwich Beams," *Journal of Sound and Vibration*, Vol. 32, April 1974, pp. 513-516.
- ⁷Yan, M. J. and Dowell, E. H., "Governing Equations for Vibrating Constrained-Layer Damping Sandwich Plates and Beams," *Journal of Applied Mechanics*, Vol. 39, Dec. 1972, pp. 1041-1047.
- ⁸Mead, D. J., "Governing Equations for Vibrating Constrained-Layer Damping Sandwich Plates and Beams," *Journal of Applied Mechanics*, Vol. 40, June 1973, pp. 639-640.
- ⁹Dahlquist, C. A., personal communication, 1973.